CHEMICAL ENGINEERING TRANSACTIONS
VOL. 56, 2017
A publication of AIDIC
The Italian Association of Chemical Engineering
Online at www.aidic.it/cet
Guest Editors: Jiří Jaromír Klemeš, Peng Yen Liew, Wai Shin Ho, Jeng Shiun Lim

ISBN 978-88-95608-47-1; **ISSN** 2283-9216
DOI: 10.3303/CET1756061

Proton Conducting Fuel Cells Using the Indium-doped Cerium Diphosphate Electrolyte

Minh-Vien Le*[,a], Dah-Shyang Tsai[b]

[a]Faculty of Chemical Engineering, Ho Chi Minh City University of Technology, VNU, 268 Ly Thuong Kiet Street, Distric 10, Ho Chi Minh City, Vietnam
[b]Department of Chemical Engineering, National Taiwan University of Science and Technology, 43, Keelung Road, Section 4, Taipei 10607, Taiwan
lmvien@hcmut.edu.vn

Proton conductivity of indium-doped cerium diphosphate (CeP_2O_7) was investigated to explore its potential for application as an electrolyte in intermediate temperature fuel cells. The In^{3+}-doped CeP_2O_7 powder was synthesized by the digestion of metal oxide in a phosphoric acid solution. The structure and ion conductivity of In^{3+} doped CeP_2O_7 were analyzed using X-ray diffraction, scanning electron microscopy (SEM), infrared spectroscopy, and electrochemical impedance spectroscopy (EIS). Under humidified conditions, the In^{3+}-doped CeP_2O_7 exhibited sufficient conductivity in the intermediate temperature range. The maximum ionic conductivity of $Ce_{0.95}In_{0.05}P_2O_7$ was 2.31×10^{-2} Scm^{-1} at 180 °C. The maximum power density of the H_2/air fuel cells fabricated using the $Ce_{0.95}In_{0.05}P_2O_7$ electrolyte (0.40 mm thickness) was 54.4 $mWcm^{-2}$ generated at 220 °C. The results indicate that $Ce_{0.95}In_{0.05}P_2O_7$ is a promising material for the fabrication of intermediate temperature fuel cells.

1. Introduction

Phosphate compounds are known for their exceptional proton conductivity. Many of these compounds are good candidates for the electrolyte in fuel cells, batteries, and sensors. In one type of phosphate containing positively polarized hydrogen atoms, such as CsH_2PO_4, loose protons are transported via the hopping (Grotthuss) mechanism within a narrow range between its superprotonic transition and decomposition temperature. In the other type of phosphates, without hydrogen in the nominal stoichiometry, protons can still be transported by H_2O, H_3O^+, OH^-, NH_4^+, etc. The superior conductivities in the intermediate temperature range of 150 - 500 °C of the second type of compounds, $M^{IV}P_2O_7$ (M=Sn, Ti, Zr, Ce), have drawn considerable research attention. This particular temperature range is of interest since it covers most of the range of operating temperatures for energy conversions and chemical processes, and a few solid proton conductors offer viable conductivity and stability for practical applications (Jin et al. 2010).
Among the $M^{IV}P_2O_7$ compounds, indium-doped SnP_2O_7 is a prominent example. (Nagao et al., 2006) reported an astonishing ion conductivity of 0.195 Scm^{-1} at 250 °C for $Sn_{0.9}In_{0.1}P_2O_7$ crystal. The same research group also documented similar proton conductivities for acceptor-doped SnP_2O_7, including 0.19 Scm^{-1} for $Sn_{0.95}Al_{0.05}P_2O_7$ at 300 °C (Tomita et al., 2007) and 0.11 Scm^{-1} for $Sn_{0.9}Mg_{0.1}P_2O_7$ at 375 °C (Genzaki et al., 2009). Wang et al. reported lower values for this diphosphate, including 4.6×10^{-2} $S.cm^{-1}$ for $Sn_{0.91}Ga_{0.09}P_2O_7$ at 175 °C (Wang et al., 2010), and 2.76×10^{-2} $S.cm^{-1}$ for $Sn_{0.94}Sc_{0.06}P_2O_7$ at 200 °C (Wang et al., 2011). These results demonstrated that the Tin diphosphate would be a promising materials for proton conducting membrane in the fuel cells operating at 175-300 °C. Similar to tin diphosphate, cerium diphosphate has also demonstrated promise as a proton conductor in the intermediate temperature range (Le et al., 2011). Sun et al. (2009) reported an ion conductivity of 0.018 Scm^{-1} at 200 °C for CeP_2O_7. Similar to acceptor doped tin diphosphate, Le's group (Le et al., 2011) reported that Mg-doped CeP_2O_7 exhibited sufficient conductivity in the intermediate temperature range, with an ion conductivity of 4.0×10^{-2} $S.cm^{-1}$ at 200 °C for $Ce_{0.9}Mg_{0.1}P_2O_7$ in humidified air with 11.4 % H_2O and power density of 40 $mWcm^{-2}$ at 240 °C.

Please cite this article as: Le M.V., Tsai D.S., 2017, Proton conducting fuel cells using the indium-doped cerium diphosphate electrolyte, Chemical Engineering Transactions, 56, 361-366 DOI:10.3303/CET1756061

The Mg doping not only raised the conductivity, but also shifted and widened the temperature range for electrolyte applications, establishing a temperature range from 160 to 280 ^{o}C.

Several studies have focused on CeP_2O_7 after the reporting of single cell using $Ce_{0.9}Mg_{0.1}P_2O_7$ as the electrolyte. Singh et al. (2012) reported a maximum conductivity value of 2.1×10^{-4} Scm^{-1} at 175 ^{o}C in air with 6 % H_2O for nondoped CeP_2O_7. Somewhat higher values have been reported elsewhere, for instance, a maximum conductivity of 6.3×10^{-3} Scm^{-1} at 90 ^{o}C in air with 12 % H_2O for $Ce_{0.9}Sr_{0.1}P_2O_7$ (Singh et al. 2013a); 2.91×10^{-2} Scm^{-1} at 190 ^{o}C, in humidified air p_{H2O} = 0.16 atm for $Ce_{0.9}Gd_{0.1}P_2O_7$ (Singh et al. 2014a); 2.24×10^{-2} Scm^{-1} at 170 ^{o}C in p_{H2O} = 0.16 atm for $Ce_{0.9}Mn_{0.1}P_2O_7$ (Singh et al. 2014b); 1.4×10^{-3} Scm^{-1} at 100 °C in a wet air atmosphere $p_{H2O} = 7.4 \times 10^3$ Pa for $Ce_{0.95}Eu_{0.05}P_2O_7$ (Wang et al. 2014). It has been shown in the literature that acceptor doping cerium diphosphates exhibit random variations in electrical conductivity, without showing any dependence on nature of the dopants (Singh et al. 2013b). The effective ionic radius of In^{3+} is 0.095 nm, is close to that of Ce^{4+} (0.087 nm), making it interesting to investigate In^{3+}-doped CeP_2O_7, which has not yet been investigated. There was a limited publication about fabricating and evaluating the operation of single cells using indium-doped cerium diphosphate as the proton conducting material.

In this study, the phase composition and microstructure of In^{3+}-doped cerium diphosphate were analysed by powder X-ray diffraction (XRD) and scanning electron microscopy (SEM). The effect of the dopant concentration on the ionic conductivity in humidified air was measured at various temperatures by electrochemical impedance spectroscopy (EIS). In addition, fuel cells were fabricated and operated while supplying humidified hydrogen and humidified air.

2. Experiments

Synthesis of cerium diphosphates started with mixing a calculated amount of ceria powder (99.9 %, Acros) with 85 % phosphoric acid (Acros) at the Ce:P molar ratio of 1:2.3, ball milled overnight, then digested at 130 °C for 24 h. The resultant yellow paste was removed from the beaker and placed in a covered alumina crucible, followed by calcination at 300 °C for 8 h. In-doped cerium diphosphate was synthesized in the same manner as for the cerium diphosphate synthesis but the CeO_2 was partially replaced by In_2O_3 (99.99 %, Sigma-Aldrich) precusours. Doped and undoped disk samples ($Ce_{1-x}In_xP_2O_7$, x=0, 0.05,0.1, 0.2) were prepared by uniaxially pressing the calcined powder into a stainless steel mold, then separately sintered at 400 °C for 8 h.

The X-ray powder diffraction (XRD) patterns of the cerium phosphate samples were recorded using an X-ray diffractometer (D2 Phaser, Bruker) equipped with a CuK_α radiation source (1.5418 Å) and nickel filter. The voltage was set at 50 kV and the current was 200 mA, while the scanned 2θ range was 15 – 70° with a step size of 0.03°. The infrared (IR) spectra were collected between 400 – 4,000 cm^{-1} using a Fourier-transform infrared spectrometer, FTIR, (Digilab FTS-3500, Biorad). The IR sample was pelletized into a powdered mixture that contained 3 wt % cerium phosphate (400 °C calcined) and 97 % KBr. The reported spectra are the average over 64 scans.

The electrochemical impedance spectroscopy (EIS) of the cerium diphosphates was measured in a sealed stainless steel chamber with tight humidity and temperature control. The sample's temperature was controlled by a heating jacket, and monitored by an inserted thermocouple. The chamber humidity was manipulated by the air flow passing a humidifier, pre-calibrated to supply nearly saturated humidified air at a specific temperature (~93 % relative humidity, <60 °C). The phosphate disk was polished and sputtered with a gold layer on both sides. The gold electrodes were pressed against two 0.2 mm gold wires, then connected to the electrical feedthroughs and then placed in the chamber. Impedance data were collected with a S1260A frequency response analyzer (Solartron Analytical) in a two-electrode configuration at zero dc bias, over 0.1 Hz – 1.0 MHz. The perturbation voltage was 10 mV for the conductive samples, and 50 mV for the less conductive samples.

The performance of the hydrogen/air fuel cell was measured by using a Keithley238 source-measure unit. The membrane-electrode assembly (MEA) was prepared by compressing a polished $Ce_{0.95}In_{0.05}P_2O_7$ pellet, which had been sintered at 400 ^{o}C for 8 h, against two circular area 1.05 cm^2 gas diffusion layers of carbon paper (GDL-10BC, SIGRACET). One side of these two carbon papers was coated with a commercially available catalyst ink (20 wt % Pt supported by Vulcan, BASF) mixed with $Ce_{0.95}In_{0.05}P_2O_7$ powder (CInP) and polytetrafluoroethylene (PTFE, 60 wt %, Aldrich). The composition of the cathode and anode coating was formulated from 50.0 wt % Pt/C catalyst powder, 35.0 wt % CInP and 15 wt % PTFE. In order to obtain homogeneous ink, an appropriate amount of glycerol solvent was added to the above mixture and mixed using mortar and pestle. The cathode and anode were dried at 150 °C to remove the glycerol solvent. The

Pt loading for both anode and cathode was calculated to be 0.6 mg.cm^{-2}. The fuel was humidified hydrogen, 50 % H_2 and 50 % N_2, while the oxidant was humidified air.

3. Result and discussion

Figure 1 shows the XRD patterns for the $Ce_{1-x}In_xP_2O_7$ pellets calcined at 400 ^oC which had been prepared from powders with a starting P/(In+Ce) molar ratio of 2.3:1 and calcined at 300 ^oC for 12 h. The main phase of the CeP_2O_7 was detected at two theta of 17.91, 20.72, 23.16, 25.44, 29.49, 34.71, 47.49 and 55.68 ^{o} in all samples which were well indexed as the cubic structure (Pa-3) by comparison with the JCPDS Card file No. 16-0584. The single phase of the sample was obtained only in the case of undoped and 5 mol % In^{3+}-doped cerium diphosphate. However, the impurity phase of CeO_2 and some other unidentified signals were detected in $Ce_{0.9}In_{0.1}P_2O_7$ and $Ce_{0.8}In_{0.2}P_2O_7$ samples. Peaks of CeO_2 were detected at two theta for 28.7, 33.3 and 56.6^o, whereas peaks of unidentified signals were detected at 26^o. The peaks of the CeO_2 residue intensified as the In^{3+} concentration increased. These results demonstrated that 5 mol % In^{3+} was the substitutable limit concentration for Ce^{4+}.

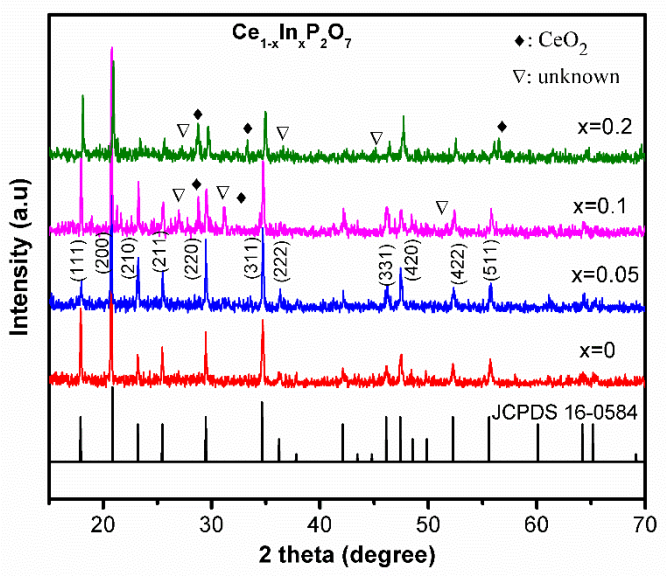

Figure 1. X-ray diffraction patterns of the $Ce_{1-x}In_xP_2O_7$ pellets calcined at 400 ^oC.

Infrared spectroscopy revealed the hydration state of the cerium diphosphates. *Figure 2 (a)* shows a comparison of the infrared spectra of the 400 °C calcined CeP_2O_7 and In^{3+}-doped CeP_2O_7 ($Ce_{1-x}In_xP_2O_7$, x= 0.05, 0.1) powders after aging for one day in air. All samples displayed a typical P-OH deformation band near 1,630-1,640 cm^{-1}, and a very broad band of O-H stretching at 2,700 – 3,700 cm^{-1}. The O-H stretching could originate from the surface water or the PO-H hydroxyl group. The strongest absorption band, around 1,057 cm^{-1}, can be attributed to asymmetric stretching of the PO_3 terminal group. The adjacent sharp absorption at 918 cm^{-1} is attributed to symmetric stretching of the PO_3 group. The two bands at 525 and 613 cm^{-1} are assigned as the deformation modes of the PO_2 and PO_3 groups (Hirai et al., 2004). We note that the 5 % In doped sample appears to be more hydrophilic than the undoped or higher Indium concentration samples. The evidence shows that the strongest intensity of O-H absorption for the CInP sample can be found at 1,057 and 3,386 cm^{-1}.

The surface morphology of the CInP pellets (Figure 2 (b)) exhibited densification, although some pores (approximately 2 μm in size) remained in the sample. The relative density of the CInP sample prepared in this study was estimated to be ~86.8 %, Being lower than that reported for Mg^{2+}-doped CeP_2O_7 (Le et al., 2011) prepared using a similar heating treatment temperature.

Humidification is critical to the proton conductivity in the cerium pyrophosphate (Le et al., 2011) by the hopping mechanism. It took a considerable amount of time to humidify the sintered cerium pyrophosphate sample disks sufficiently so that the conductivity reached a steady-state value. Nearly 1 day was needed to obtain a steady-state humidified sintered disk at 80 ^{o}C in the impedance measurement chamber. However, the time it took to reach the steady-state value was shorter as the measurement temperature increased.

Figure 3(a) shows Nyquist plots of the CInP pellets, measured in moist air with P_{H2O} = 0.114 atm, at 80, 100, 120 and 140 ^{o}C. As can be seen, the CInP pellets become more conductive with increasing temperature.

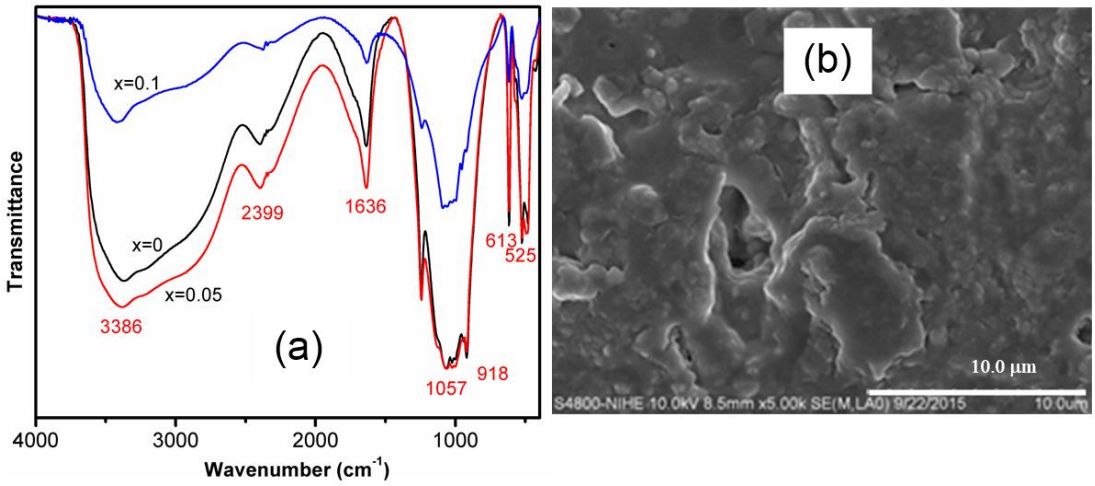

Figure 2. (a) Infrared spectra of the 400 ℃ calcined $Ce_{1-x}In_xP_2O_7$ powders (x=0, 0.05, 0.1) and (b) microstructure of the 400 ^{o}C-sintered CInP disk

The steady impedance data were fitted to an equivalent circuit (see the insert to Figure (3a)), where R_{gi} and R_{gb} indicate the resistance of bulk and grain boundary contribution, respectively. The value of the proton conductivity σ is calculated as follows: $tA^{-1}(R_{gi}+R_{gb})^{-1}$, where t is the thickness of the disk and A is the disk area. For comparative purposes, the values of the proton conductivity, measured at P_{H2O} = 0.114 atm, are plotted versus temperature in Figure 3(b). A dashed line for 1.0×10^{-2} Scm^{-1} is also drawn to mark the lower bound for electrolyte applications. We note a tremendous similarity between the low temperature conductivities of the doped and undoped samples, which show a nearly parallel temperature dependence below 140 °C. The parallel proton conductivities at temperatures lower than 140 °C suggest a similar proton conduction mechanism at work in the doped and undoped CeP_2O_7 in the low temperature regime. When the temperature became higher than 140 °C, the temperature dependence of the samples began to differ from each other. As a result, the undoped CeP_2O_7 would be more suitable for low-temperature applications, as shown by the conductivity σ, which had a value larger than 0.01 S cm^{-1} in the range from 120 – 190 °C. Moreover, Figure 4 (b) shows that the maximum proton conductivity of $Ce_{0.95}In_{0.05}P_2O_7$ was measured to be 2.31×10^{-2} S cm^{-1} at 180 °C, but this decreased at higher temperatures, 2.24×10^{-2} S cm^{-1} at 200 °C and 1.16×10^{-2} S cm^{-1} at 220 °C. The maximum conductivity of $Ce_{0.95}In_{0.05}P_2O_7$, 2.31×10^{-2} S cm^{-1} at 180 °C was higher than that of CeP_2O_7, 2.2×10^{-2} S cm^{-1} at 180 °C. The maximum conductivities of $Ce_{0.9}In_{0.1}P_2O_7$ and $Ce_{0.8}In_{0.2}P_2O_7$ were 1.44 $\times10^{-2}$ S cm^{-1} at 180 °C and 1.02 $\times10^{-2}$ S cm^{-1} at 160 °C. The applicable temperature range of the $Ce_{0.95}In_{0.05}P_2O_7$ sample ($\sigma \geq 1.0\times10^{-2}$ S cm^{-1}) was 120 – 220 °C, wider than the others. It can be concluded that the 400 °C-sintered CInP sample had the most conductive composition in this investigation. The performance of single cell Pt/C+ CInP| CInP |Pt/C+ CInP samples using a 0.40 mm thick electrolyte was evaluated at various temperatures under humidified H_2/air fuel cell conditions (Figure 4(a)). The open-circuit voltages (OCVs) at the tested temperatures were between 0.60 and 0.65 V, considerably lower than the theoretical value of ~1.1 V. The low OCVs were due to the physical leakage of hydrogen gas through the electrolyte which contributed to the porosity of the electrolyte membrane, as our sensor detected a low hydrogen of low concentration at the cathode side. As can be seen from Figure 4a, the cell performance was strongly dependent on the operating temperature. The peak power density increased in value with the increasing operating temperature, reaching a maximum value of 54.4 mW cm^{-2} at 220 ^{o}C, and then decreasing to 33 mWcm^{-2} at 260 °C. Deducing from this, the power density of this intermediate temperature fuel cell was strongly influenced by the conductivity of the electrolyte, which followed the same trend, increase-then-decrease, as the proton conductivity. Thus, it is concluded that this fuel cell is suitable for the operation at around 220 °C.

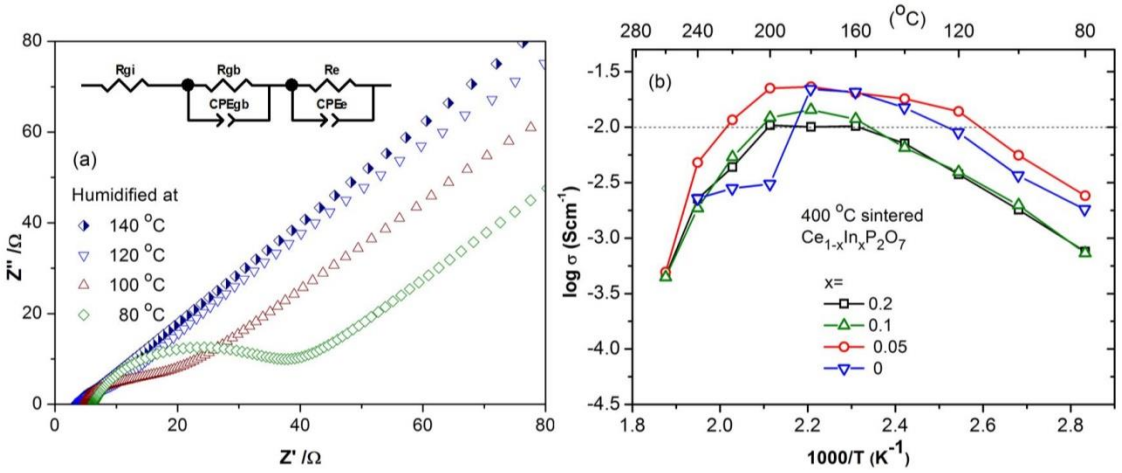

Figure 3. Variation in (a) impedance and (b) conductivity of 400 °C-sintered $Ce_{1-x}In_xP_2O_7$ vs. temperature under humidified conditions.

Figure 4 (b) shows the cell voltage and power density curve of the Pt/C+ CInP| CInP |Pt/C+ CInP fuel cells in relation to the differences in the thickness of the electrolyte, from 0.36 to 0.51 mm. The value of the peak power density increased as the thickness of the electrolyte increased from 0.36 to 0.40 mm, reaching a maximum value of 54.4 $mWcm^{-2}$ with a thickness of 0.44 mm, and decreasing to 33 $mWcm^{-2}$ when the thickness was 0.51 mm. The decrease in the power density value when the thickness of the electrolyte was larger than 0.40 mm was due to the increasing ohmic resistance. The performance of the $Ce_{0.95}In_{0.05}P_2O_7$ cell with an electrolyte thickness of 0.40 mm was 54.4 $mWcm^{-2}$ at 220 °C, which was higher than that of the CeP_2O_7 cell, reported by Sun et al. (2009), which was 25 $mWcm^{-2}$ at 200 °C, that of the $Sn_{0.94}Sc_{0.06}P_2O_7$ cell reported by Wang et al. (2011), which was 25 $mWcm^{-2}$ at 150 °C, or that of the $Sn_{0.91}Ga_{0.09}P_2O_7$ cell , which was 22 $mWcm^{-2}$ at 175 °C, reported by Wang et al. (2010). However, these peak power values are much lower than that of the $Sn_{0.9}In_{0.1}P_2O_7$ cell, of 264 $mWcm^{-2}$ at 250 °C (Heo et al., 2006) and that of the cell fabricated using a composite electrolyte of H_3PO_4-doped PBI/SAPO, which was 439.6 $mWcm^{-2}$ at 200 °C (Jin et al., 2011). The low power of cell could result from the less-ideal cell potential and thick electrolyte membrane.

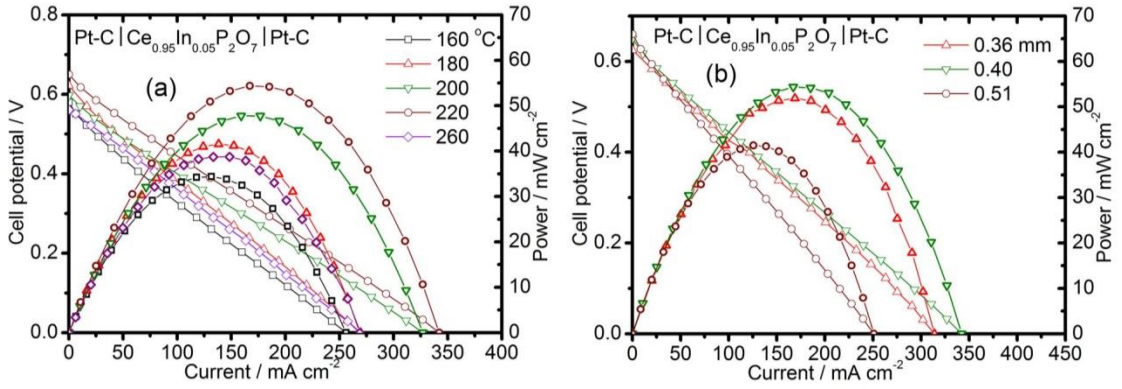

Figure 4. (a) Cell voltage and power density of fuel cells vs. temperature under humidified conditions and (b) with different electrolytes thicknesses at a temperature of 220 °C under humidified conditions

4. Conclusions

This study has investigated the proton conductivity and fuel cell performance of In-doped CeP_2O_7 in the intermediate temperature range. The $Ce_{0.95}In_{0.05}P_2O_7$ was identified as the optimum composition of cerium diphosphate for electrolyte applications. The $Ce_{0.95}In_{0.05}P_2O_7$ disk, sintered at 400 °C, exhibited a conductivity higher than 0.01 S cm^{-1} in moist air P_{H2O} = 0.114 atm between 120 – 220 °C. The maximum conductivity was 2.31×10^{-2} S cm^{-1} at 180 °C, higher than that of CeP_2O_7 2.2×10^{-2} S cm^{-1} at 180 °C, which

can be compared to that of Mg-doped cerium diphosphate (Le et al.; 2011). The maximum power density of 54.4 mW cm^{-2} at 220 ^oC was generated for fuel cells fabricated using the $Ce_{0.95}In_{0.05}P_2O_7$ electrolyte. The fuel cell performance can be improved by decrease the thickness of CnIP electrolyte.

Acknowledgement

This research has been funded by the Department of Science and Technology (DOST, Hochiminh City, Vietnam) from 2014-present, under grant number 286/2014/HĐ-SKHCN.

References

Genzaki K., Heo P., Sano M., Hibino T., 2009, Proton conductivity and solid acidity of Mg-, In-, and Al-doped SnP_2O_7, J. Electrochem. Soc. 156, 806-810.

Heo P., Shibata H., Nagao M., Hibino T., Sano M., 2006, Performance of an intermediate temperature fuel cell using a proton conducting $Sn_{0.9}In_{0.1}P_2O_7$ electrolyte, J. Electrochem. Soc. 153, 897-901.

Hirai H., Masui T., Imanaka N., Adachi G., 2004, Characterization and thermal behavior of amorphous rare earth phosphates, Journal of Alloys and Compounds, 374, 84–88.

Jin Y.C., Lee B., Hibino T., 2010, Development and application of SnP_2O_7-based proton conductors to intermediate temperature fuel cells, J. Jpn. Petrol. Inst. 53, 12-23

Jin Y.C., Nishida M., Kanematsu W., Hibino T., 2011, An H_3PO_4-doped polybenzimidazole /$Sn_{0.95}Al_{0.05}P_2O_7$ composite membrane for high-temperature proton exchange membrane fuel cells, Journal of Power Sources, 196, 6042-6047.

Le M.V, Tsai D.S., Yang C.Y., Chung W.H., Lee H.Y., 2011, Proton conductors of cerium pyrophosphate for intermediate temperature fuel cell, Electrochim. Acta 56, 6654-6660.

Nagao M., Takeuchi A., Heo P., Hibino T., Sano M., Tomita A., 2006, A proton conducting In^{3+}-doped SnP_2O_7 electrolyte for intermediate temperature fuel cells, Electrochem. Solid-State Lett. 9, 105-109.

Singh B., Im H., Park J., Song S., 2012, Electrical Behavior of CeP_2O_7 Electrolyte for the Application in Low-Temperature Proton-Conducting Ceramic Electrolyte Fuel Cells, J. Electrochem. Soc., 159, F819-F825.

Singh B., Im H., Park J.Y, Song S., 2013a, Studies on Ionic Conductivity of Sr^{2+}-Doped CeP_2O_7 Electrolyte in Humid Atmosphere, J. Phys. Chem. C, 117, 2653–2661.

Singh B., Jeon S.Y., Im H.-N., Park J.-Y., Song S.-J., 2013b, Electrical conductivity of M^{2+}-doped (M = Mg, Ca, Sr, Ba) cerium pyrophosphate-based composite electrolytes for low-temperature proton conducting electrolyte fuel cells, Journal of Alloys and Compounds 578, 279–285.

Singh B., Jeon S.Y., Kim J.H., Park J.Y, Bae C., Song S.J., 2014a, Ionic Conductivity of Gd^{3+} Doped Cerium Pyrophosphate Electrolytes with Core-Shell Structure, Journal of The Electrochemical Society, 161, 464-472.

Singh B., Kim J.H., Jeon S.Y., Park J.Y., Song S.J., 2014b, Mn^{2+}-Doped CeP_2O_7 Composite Electrolytes for Application in Low Temperature Proton-Conducting Ceramic Electrolyte Fuel Cells, Journal of The Electrochemical Society, 161, 133-138.

Sun X., Wang S., Wang Z., Ye X., Wen T., Huang F., 2009, Proton conductivity of CeP_2O_7 for intermediate temperature fuel cells. Solid state Ionics 179, 1138-1141.

Tomita A., Kajiyama N., Kamiya T., Nagao M., Hibino T., 2007, Intermediate temperature proton conduction in Al^{3+}-doped SnP_2O_7, J. Electrochem. Soc. 154, 1265-1269.

Wang H., Liu J., Wang W., Ma G., 2010, Intermediate temperature ionic conduction in $Sn_{1-x}Ga_xP_2O_7$, J. Power Sources 195, 5596-5600.

Wang H., Zhang H., Xiao G., Zhang F., Yu T., Xiao J., Ma G., 2011, Ionic conduction in $Sn_{1-x}Sc_xP_2O_7$ for intermediate temperature fuel cells, J. Power Sources 196, 683-687.

Wang H., Sun L., Luo C., Fan S., 2014, Studies on Ionic Conduction in $Ce_{0.95}Eu_{0.05}P_2O_7$ at Intermediate Temperatures, Bull. Korean Chem. Soc. 35, 1465-1468.